Fermi National Accelerator Laboratory

FERMILAB-Pub-81/33-EXP
7840.108

(Submitted to Nucl. Instrum. Methods)

MEASUREMENTS OF RADIAL AND LONGITUDINAL HADRON SHOWER DEVELOPMENT AT 300 GeV

P. J. Gollon, M. Awschalom, S. Baker, L. Coulson, C. Moore, and S. Velen

April 1981

Operated by Universities Research Association Inc. under contract with the Energy Research and Development Administration

MEASUREMENTS OF RADIAL AND LONGITUDINAL HADRON SHOWER DEVELOPMENT AT 300 GeV

P.J. Gollon,* M. Awschalom, S. Baker, L. Coulson, C. Moore and S. Velen

Fermi National Accelerator Laboratory

Batavia, Illinois 60510

We present the first measurements of the average energy deposition (as measured by small scintillators) in hadron showers produced by 300 GeV protons (as measured by small scintillators) as a function of position in Al, Fe and Pb multiplate calorimeters. Sample energy deposition spectra are also presented for the first time. These measurements may be used as "benchmark" comparisons for Monte Carlo hadron cascade programs.

Work performed under the auspices of the U.S. Department of Energy.

*Present address Brookhaven National Laboratory, Upton, N.Y. 11973

I. Introduction

Since their introduction into experimental high energy physics from cosmic ray work roughly twenty years ago, ionization calorimeters have been required to provide increasing amounts of information at ever higher energies.[1] The state-of-the-art calorimeter now in use or being planned is typically a segmented device which must simultaneously provide accurate information on the positions and energies of several or many particles (or jets of particles) incident upon it from a single interaction.[2]

As these devices have grown more complicated and expensive, their designers have increasingly turned to Monte Carlo programs[3] to predict the performance of a particular design before building a prototype. Similar programs are also used, for example, to predict energy deposition due to beam losses in superconducting coils of accelerator magnets,[4] and for the design of accelerator radiation shielding.[5] These programs are usually based on measured inclusive cross sections for pions and nucleons at energies from tens of MeV to a few hundred GeV. Such programs make many simplifying assumptions concerning the propagation of the hadronic and electromagnetic cascades, the deposition of energy by these cascades, and the conversion of this energy into light in scintillators. We therefore felt that the accuracy of such Monte Carlo cascade programs could best be tested by comparison with detailed measurements of the spatial development of hadron cascades in several materials at very high energy. We believe that the measurements reported here provide just such a benchmark.

II. Apparatus

These measurements were made in a 300 GeV diffracted proton beam in the M2 beamline at Fermilab. The apparatus shown in Fig. 1 was placed in a well-collimated narrow beam of about 10^6 particles/second. The trigger logic ($B_1 \cdot B_2 \cdot [B_2<\hat{2}] \cdot \bar{V} \cdot \overline{VH}$) selected only beam particles which were unaccompanied by another beam particle in the same or in either adjacent rf bucket. The 3 mm diameter beam so selected struck the Fe, Al or Pb "converter" shown in Fig. 1. The calorimeter behind the converter consisted of 10 cm thick plates (of the same material as the converter) spaced 5 cm from each other. Six air light guide "finger" scintillation counters (1 cm high x 0.5 cm wide x 1 cm thick) were arranged on a movable platform to horizontally scan the width of the calorimeter, measuring the energy deposited in the finger counters for each recorded event.[6]

"Shower" events, intended to be those in which a shower started in the 5 cm thick converter (10 cm thick in the case of Al), were selected by requiring more than twice single-particle signals from shower counters S_1 and S_2 (3.2 cm square) directly behind the converter, in coincidence with an incident beam particle.

Signals from all six finger counters were recorded only for those events in which at least one of the finger counters had a signal at least 0.2 to 0.3 that of a minimum ionizing particle. This allowed us to get a reasonable sampling of the larger energy deposition events at some distance from the shower axis. Prescaling by up to a factor of four $[(F_1 + F_2)/2^m + (F_3 + F_4)/2^n + (F_5 + F_6)/2^k]$ was used to keep triggers from the finger counters nearest the shower maximum from dominating the recorded data. Latch bits on discriminators and prescalers allowed us to determine the triggering conditions for each recorded event.

The triggering requirements thus selected events in which exactly one incoming particle produced at least two particles in the shower counters and the resulting shower produced a prescaled signal above a low threshold in at least one finger counter.

The energy calibration was determined by fitting the spectrum produced by protons cleanly traversing the counter with a Landau distribution (for energy deposition) convoluted with a Gaussian (for photomultiplier resolution and noise). A typical counter, such as the one whose calibration fit is shown in Fig. 2, had an energy resolution (FWHM) of about 30%. This was sufficient to distinguish between 1, 2 or 3 particles traversing a counter simultaneously, as shown in Fig. 3. The position of the Landau peak prior to convolution (i.e. the most probable energy deposition with perfect resolution) defines the pulse height of an "equivalent particle" (EP). This quantity is unaffected by the relativistic rise of dE/dx with beam energy.[7]

When the finger counters were on the beamline, they produced signals ranging up to ~ 30 equivalent particles during nearly every "shower". As the counters were moved away from the beamline, the fraction of showers producing sizeable signals declined dramatically. For example, at a radius of 20 cm and a depth of 30 cm (in Pb or Fe), only one shower in approximately 200 produced a signal in a finger counter greater than about half an EP.

Scans were made starting from a point 1 cm away from the beam line, passing through the beam line and continuing out as far as 28 cm for the Al plates. The assembly of 6 finger counters was then moved downstream 5 slots, so the slot that was scanned by the last finger during one radial scan was then scanned by the first finger during the next scan. The reproducibility of the scan results under these circumstances indicates that $\lesssim$ 10% error resulted from the

triggering system used for the Al and Pb measurements. (The Fe data were handled differently, as discussed below.) All finger counters were calibrated by beam protons at each longitudinal position before and after each radial scan.

III. Data Analysis and Results

The first step in the data analysis, after rejecting events with inconsistent latch and counter ADC data was the imposition of a software cut on the shower counters (5 EP) well above the level used in the triggering logic. This ensured a rather clean sample of hadron showers originating in the converter. (The remaining backsplash contamination[8] from first interactions occurring downstream of the shower counters should be reproduced by the cascade programs being tested.)

The individual energy deposition signals in each finger counter were then histogrammed separately according to the following scheme. First, if a finger counter had a signal above its discriminator threshold, and its associated prescaler fired, then the signal from that finger was capable of initiating the recording of the entire event. Such signals were placed in a "latch" spectrum for each finger. Such a spectrum (Fig. 4b) represents the as yet unnormalized high energy tail of the energy deposition spectrum for a particular point inside the dump.

Second, for each finger meeting the above criteria (say F_1), all the other finger counters except the one sharing a prescaler with F_1 (i.e. F_3 - F_6, but not F_2) had their signals entered into their individual "unbiased" histograms. Such histograms (Fig. 4a) are, in the absence of correlations between fingers, just random samplings of the entire energy deposition spectrum of the shower at various points in the dump. Note that the above scheme causes, for

suitable combinations of signals on the finger counters, a given finger counter's signal be entered into its unbiased histogram, its latch histogram, both, or neither, as shown in Table 1.

Note how few events there are with large energy deposition in the "unbiased" spectrum in Fig. 4a. Fig. 4b shows the "latch" spectrum for the same position, with much better statistics at higher energies, but with no events below the finger discriminator threshold. These histograms are individually normalized to the number of showers starting in the converter by correcting for deadtime, prescaling factors, and the effects of the deliberate selection of events with large energy deposition. The latch and unbiased histograms of Fig. 4a and 4b are shown properly normalized in Fig. 4c. The normalized histograms are then "spliced" together at an appropriate point of overlap (shown by arrow) to form the completed pulse height spectrum at each measured location in the calorimeter.

Finally, all events in a histogram with energy deposition (E_{dep}) less than E_{Lo} = 0.3 EP (0.2 EP for Pb) have E_{dep} set equal to zero. This collapses the large peak at zero energy deposition (whose width is mostly due to noise) into a delta function, and prevents minor drifts in the calibration and changes in the noise level from dominating the spectrum average. Further, any signals greater than E_{hi} = 60 EP (35 EP for Al) were set equal to E_{hi} in order to treat those few events which would overload the electronics in a known way. The mean of each pulse height spectrum so obtained is then the average energy deposited in the finger counter per shower starting in the converter block.

Figure 5 shows representative pulse height spectra for various locations in the Pb calorimeter. The transition from many particles

traversing the 0.5 cm^2 counter at small radii to occasional feeble energy depositions at large radii is quite dramatic. The same general trend is observed in the Al and Fe shower data.

Data from the iron calorimeter were analyzed in much the same manner as outlined above, but with some important differences. Because of instrumental problems it was not possible to splice the "unbiased" and "latch spectra" as was done form the other two materials. Rather, an unbiased spectrum for each counter was approximated in the analysis by accepting for a finger counter histogram those events for which the counters immediately downstream had signals above a specified level (0.8 EP).

Figure 6 shows the cascade development curves for all three calorimeter materials. The short radiation length and resulting very rapid shower development in lead prevent us from resolving the shower maximum in this material with our coarse (10 cm) plate spacing. Figure 7 shows the Al and Pb data of Fig. 6 plotted as a function of radius for constant depth. These perspective drawings allow one to better appreciate the very concentrated nature of the energy deposition in the shower. The rapid radial falloff of energy deposition shown in these figures results from both radial attenuation and geometric 1/r dilution.

We were also able to examine the question of correlations in energy deposition between two locations at the same radius, but different depths in the dump. A simple measure of this is the probability that two successive 0.5 cm^2 finger counters F_i and F_{i+1} have significant signals (taken to be $\geq$ 0.8 EP) in them. Figure 8 shows this data for all three materials. It is clear that these correlations are not significant at radii past a few cm, and decrease fairly rapidly with depth.

Summary

We have presented detailed measurements of the average energy deposition by high energy protons in aluminum, iron and lead multiplate calorimeters. This data is suitable for use as a benchmark for all Monte Carlo hadron cascade programs. The measured energy deposition spectra at various locations in the calorimeter provide an even more detailed test of the analogue Monte Carlo programs which are capable of calculating such quantities.

Acknowledgment

It is a pleasure to acknowledge the significant efforts by M. Atac, R. Shafer and D. Theriot in developing and building the apparatus. The construction and running of the experiment benefitted from the enthusiasm and skills of L. Grumboski, J. Larson, D. Voy, and C. Zonick. Data analysis was greatly assisted by the efforts of D. Cossairt.

Table I.

Illustrative examples of how the pattern of finger counter and prescaler "latch" hist determine how to histogram a given event. Note that each pair of counters (F_1 and F_2; F_3 and F_4; F_5 and F_6) share a prescaler.

	Finger Counter					
	F1	F2	F3	F4	F5	F6
Above threshold	X			X		
Prescaler fired		X				
Place in "latch" histogram	X					
Place in "unbiased" histogram			X	X	X	X
Above threshold	X			X		
Prescaler fired		X		X		
Place in "latch" histogram	X			X		
Place in "unbiased" histogram	X	X	X	X	X	X
Above threshold			X	X		
Prescaler fired				X		
Place in "latch" histogram			X	X		
Place in "unbiased" histogram	X	X			X	X

References

1. See, for example, "Principles and Application of the Ionization Calorimeter," V.S. Murzin, in Progress in Elementary Particle and Cosmic Ray Physics, Vol. IX, 1967 (North Holland); and Proc. Calorimeter Workshop, May 1975 (Fermilab) and other references therein.

2. B.C. Barish et al., Nucl. Instrum. and Methods 130 (1975) 49; A. Sessoms et al., Nucl. Instrum. and Methods 161 (1979) 371; and B.T. Yost et al, IEEE Trans. Nucl. Sci. NS-26 (1979) 105.

3. T.A. Gabriel and J.D. Amburgey, Oak Ridge Report ORNL-TM-4349 (1973)1; also see papers by T.A. Gabriel, A. Van Ginneken, and by W.V. Jones in Proc. Calorimeter Workshop, May 1975 (Fermilab).

4. A. Van Ginneken, NAL-TM-685(1976); and G. Bozoki, ISABELLE TN-108 (1979).

5. A. Van Ginneken and M. Awschalom "High Energy Particle Interactions in Large Targets", Fermilab (1975).

6. A somewhat similar technique was used at 10 GeV by B. Friend, et al. Nucl. Instrum. and Methods 136 (1976) 505. Profiles with coarser resolution were measured at energies up to 86 GeV by D. Bollini et al., Nucl. Instrum. and Methods 171 (1980) 237.

7. R.M. Sternheimer and R.F. Peierls, Phys. Rev. B3 (1971) 3681 and B.C. Barish et al., Nucl. Instrum. and Methods 130 (1975) 49.

8. R.W. Ellsworth et al., Proc. Calorimeter Workshop (Fermilab) May 1975, p.201.

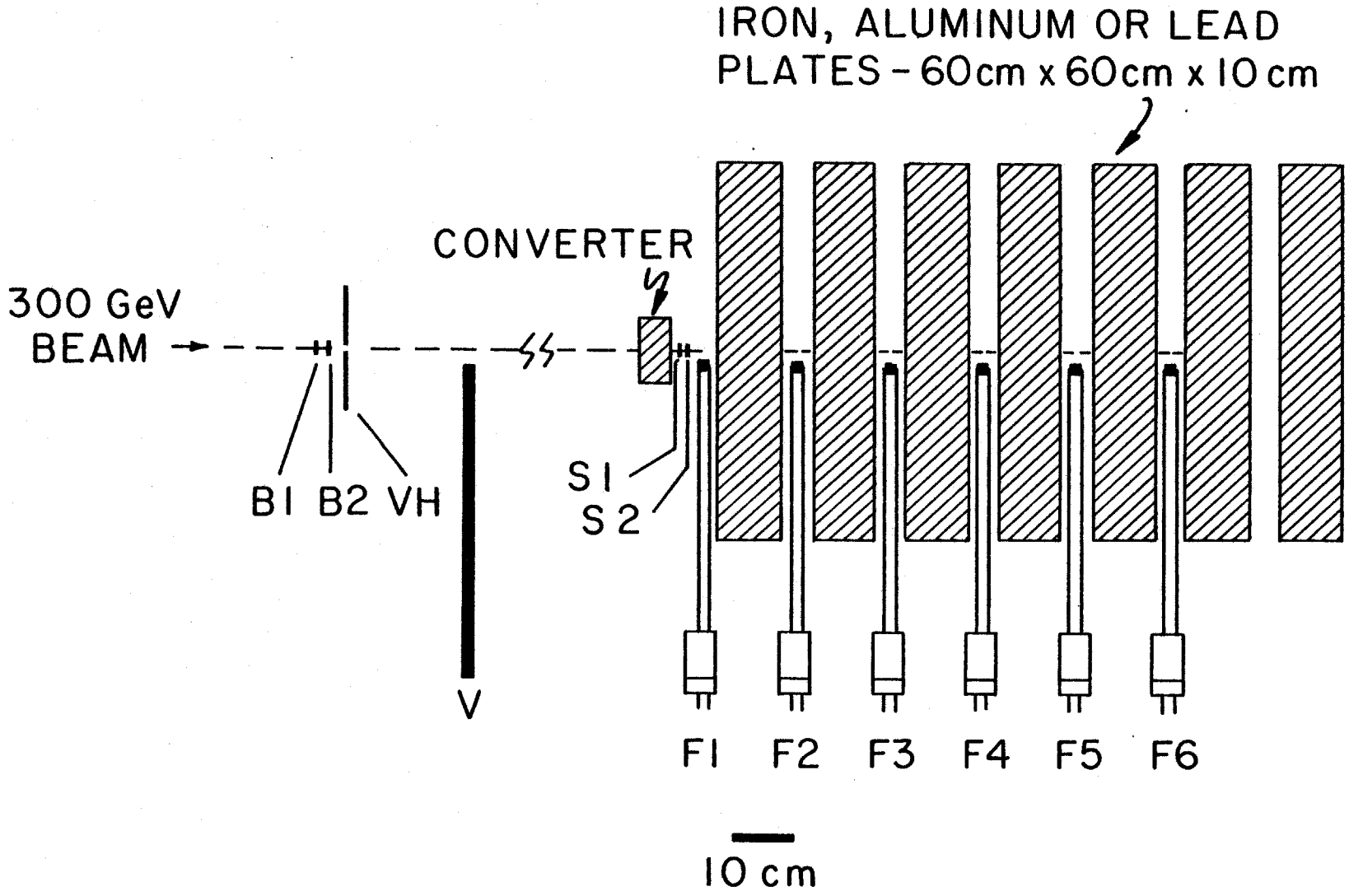

1. Plan view of the apparatus used. The trigger logic (discussed in the text) defined events in which exactly one incoming particle produced at least two particles in the converter and the resulting shower produced a prescaled signal above a low threshold in at least one finger counter Veto counters V and VH protected against incident stray particles.

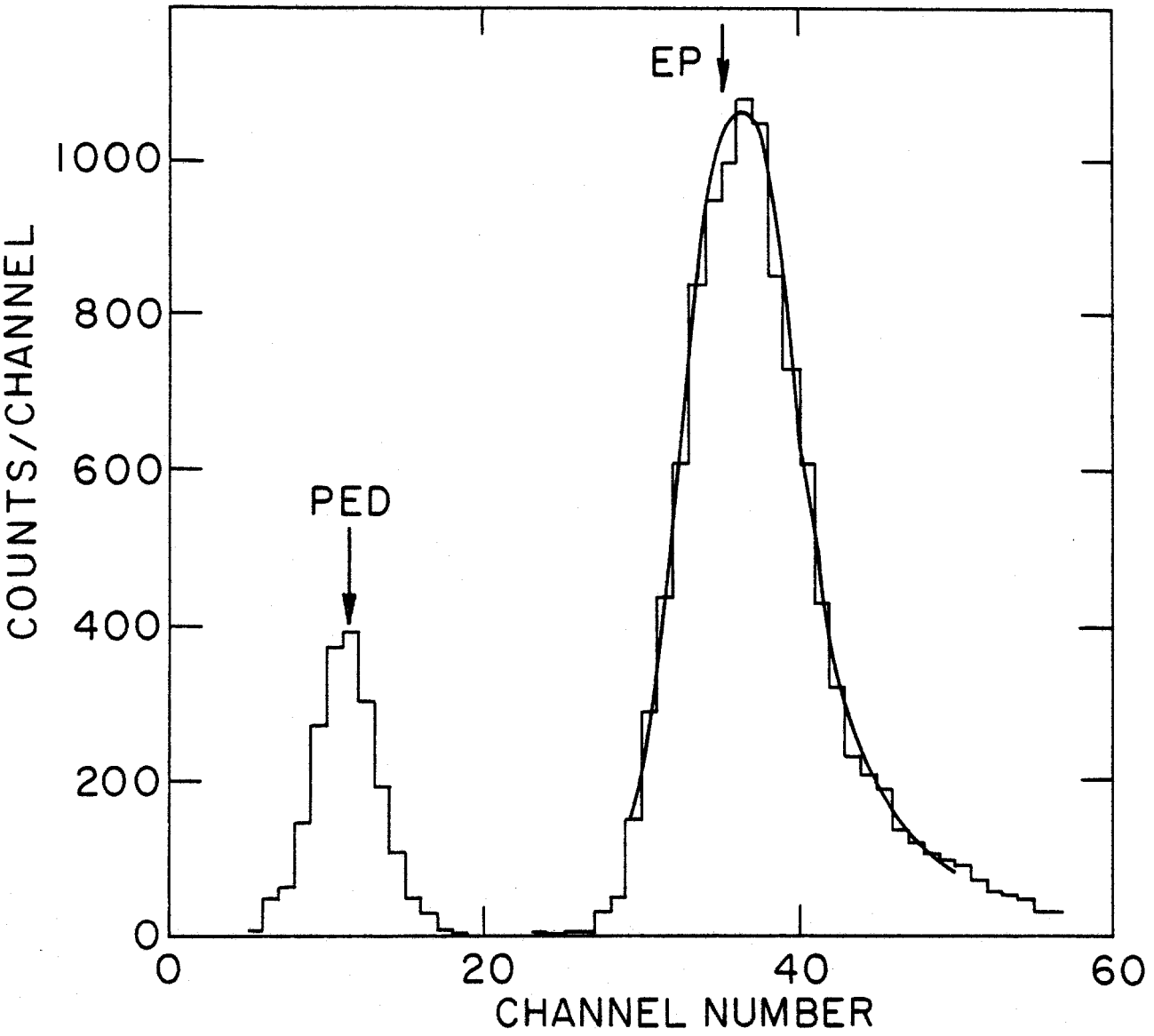

2. Typical calibration spectrum for a finger counter. The "PED" peak on the left is the pedestal obtained with no particles traversing the counter; its centroid (arrow) defines zero energy. The right histogram is produced by protons traversing the counter; the curve is a Landau convoluted with a Gaussian representing counter noise and PMT resolution. The arrow "EP" shows where the peak (most probable value of energy deposition) would be if there were no counter noise or imperfect PMT resolution smearing out the asymmetrical Landau distribution. This defines the pulse height of an "equivalent particle" that sets the energy scale of the measurements.

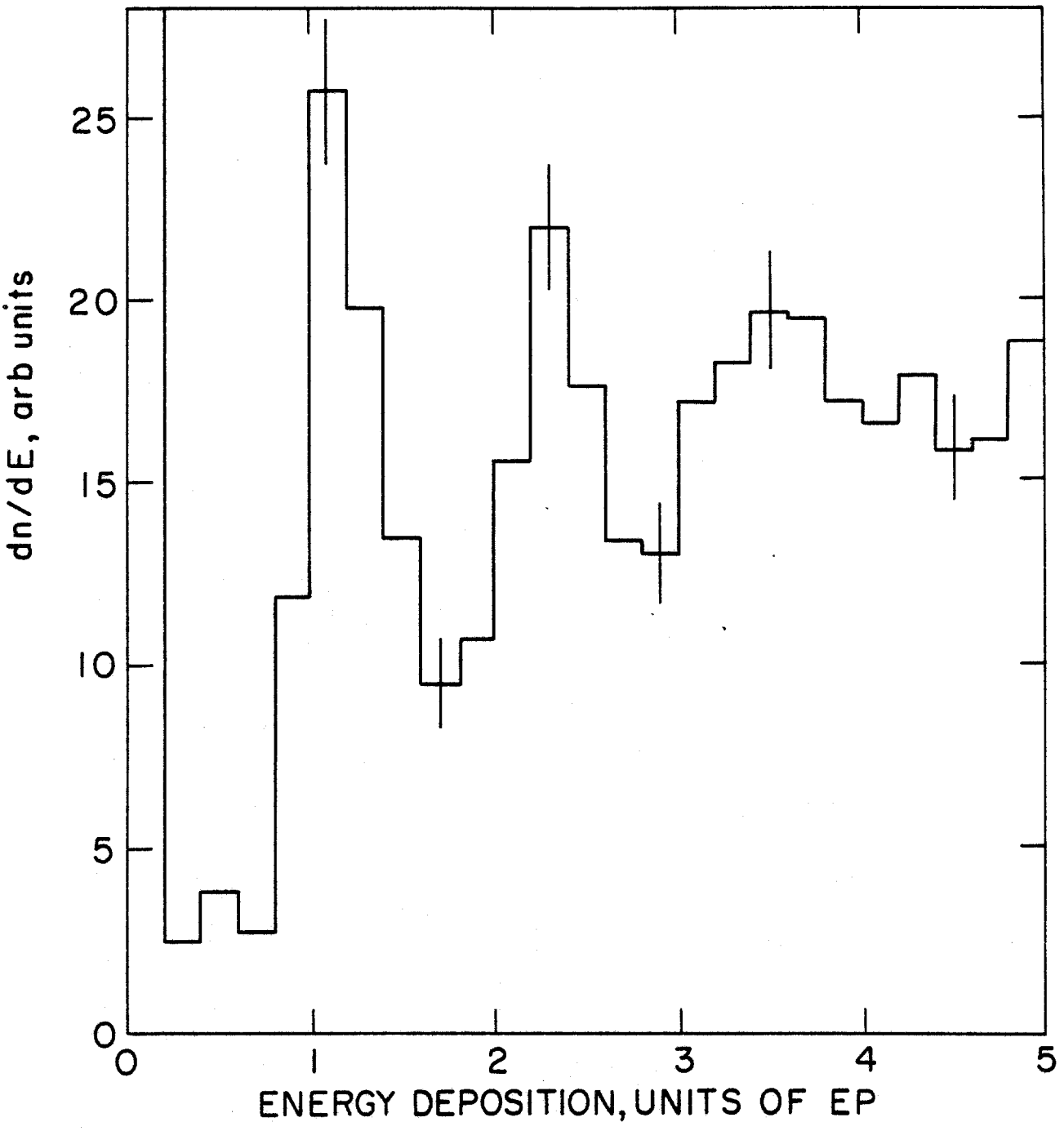

3. The lower end of the shower event pulse height spectrum on the beamline at a depth of 10 cm in the aluminum calorimeter. At such a shallow depth we are able to distinguish between 1, 2 or 3 charged particles simultaneously traversing a finger counter. The systematic shift of the sum peaks toward higher than nominal energy is due to the asymmetrical nature of the single particle spectrum, Fig. 2.

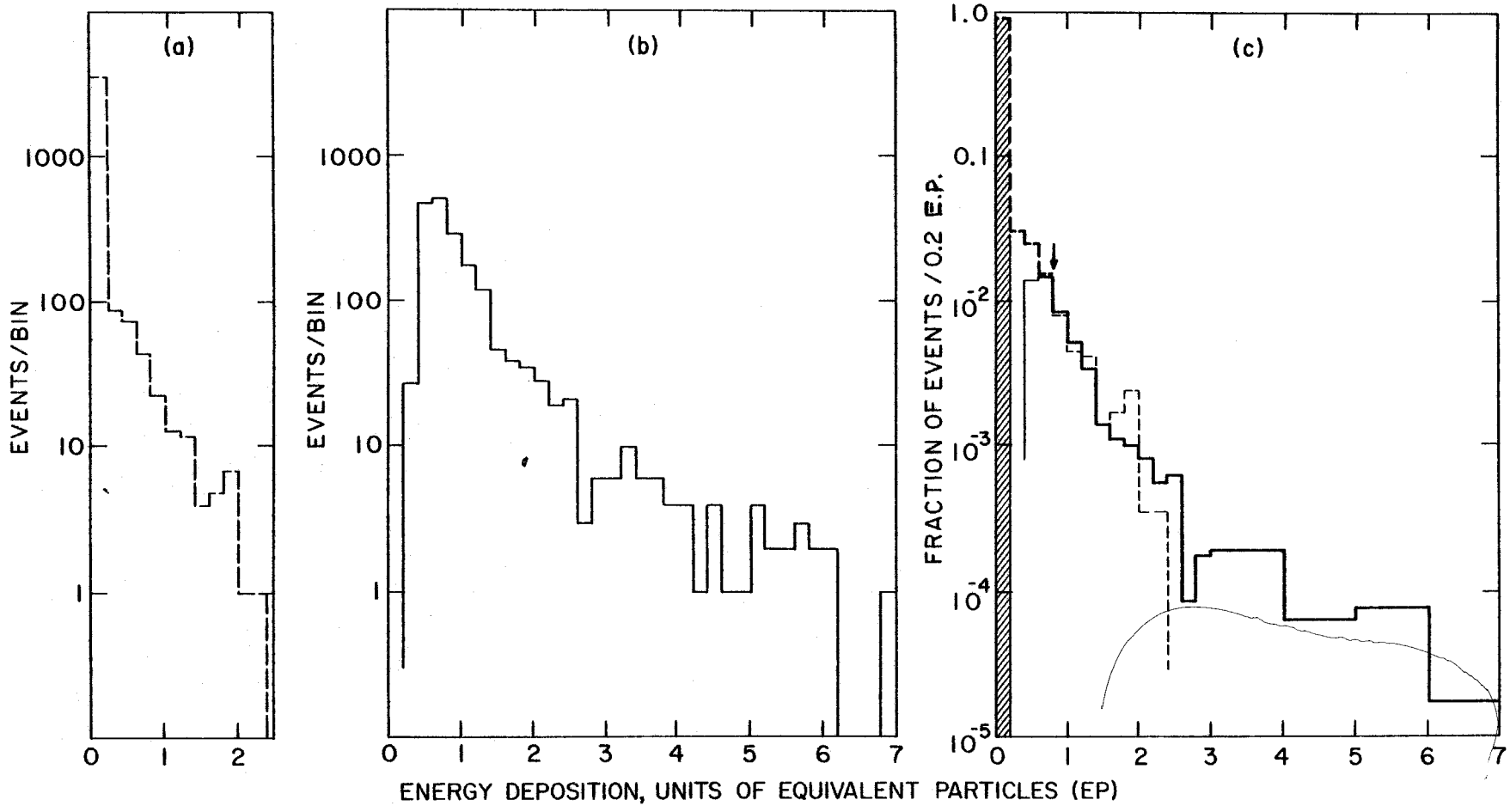

4. (a) A typical unnormalized "unbiased" histogram showing many events extending down to the noise level of the counters.

(b) The unnormalized "latch" histogram for the same counter, showing signals above the threshold discriminator level extending with good statistics, to the high energy tail of the spectrum.

(c) The histograms of (a) and (b), properly normalized. They are "spliced" together at the arrow to yield a completed spectrum (heavy dashed and solid lines). The shaded area is presumed to be due to counter noise and is replaced by signal values identical to zero. The higher energy bins have been averaged in groups of 5 to reduce statistical fluctuations.

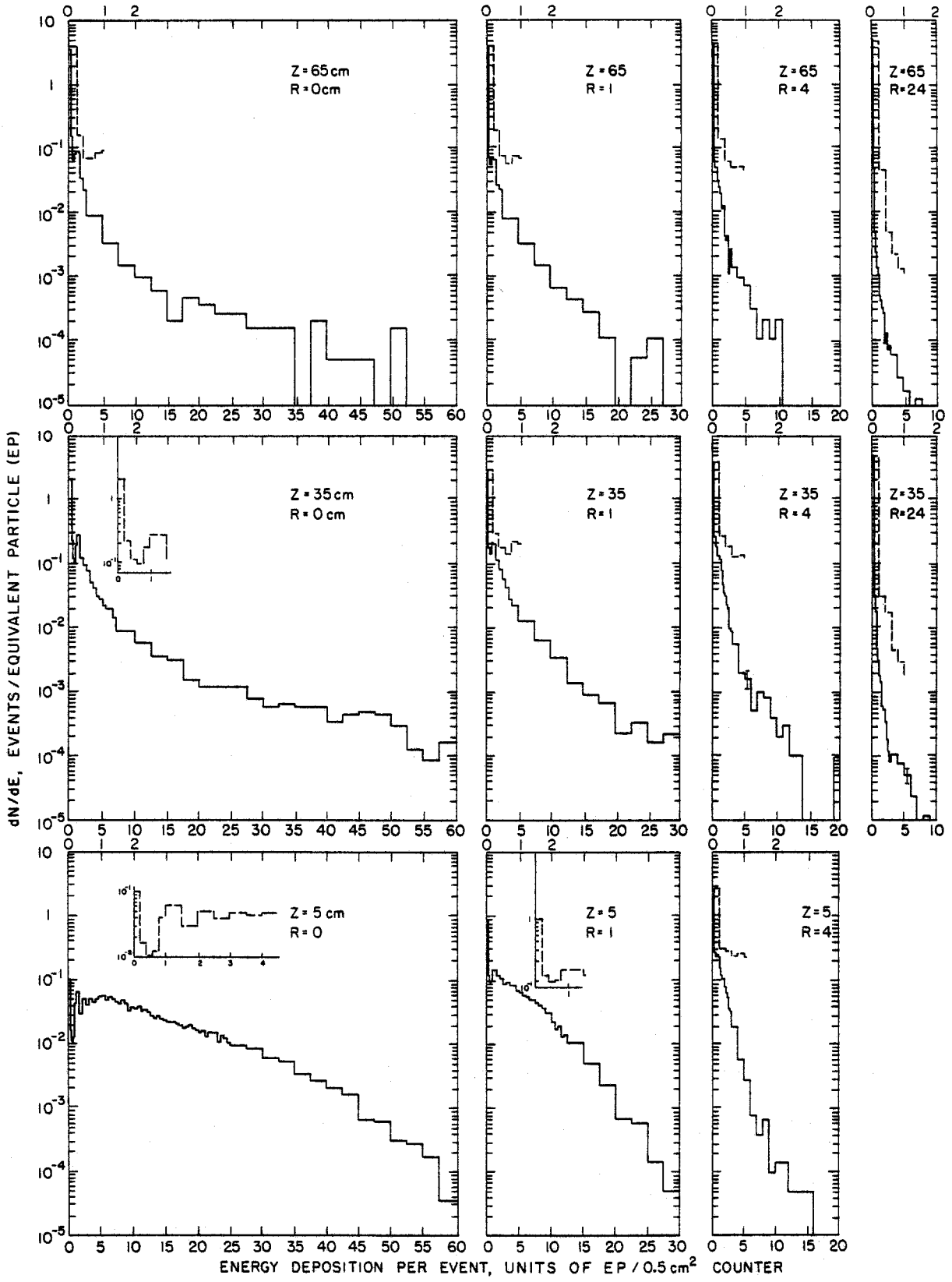

5. Sample normalized finger counter pulse height spectra for various locations in the Pb dump. The solid histograms refer to the lower abscissas; the dashed histograms (upper abscissas) and insets give an expanded version of the low-energy end of the same data. The spectra at small radii are dominated by events with energy deposition in the 0.5 cm^2 counter of tens of times that of a single particle; the spectra at large radii consist almost exclusively of events depositing less energy than a single particle would.

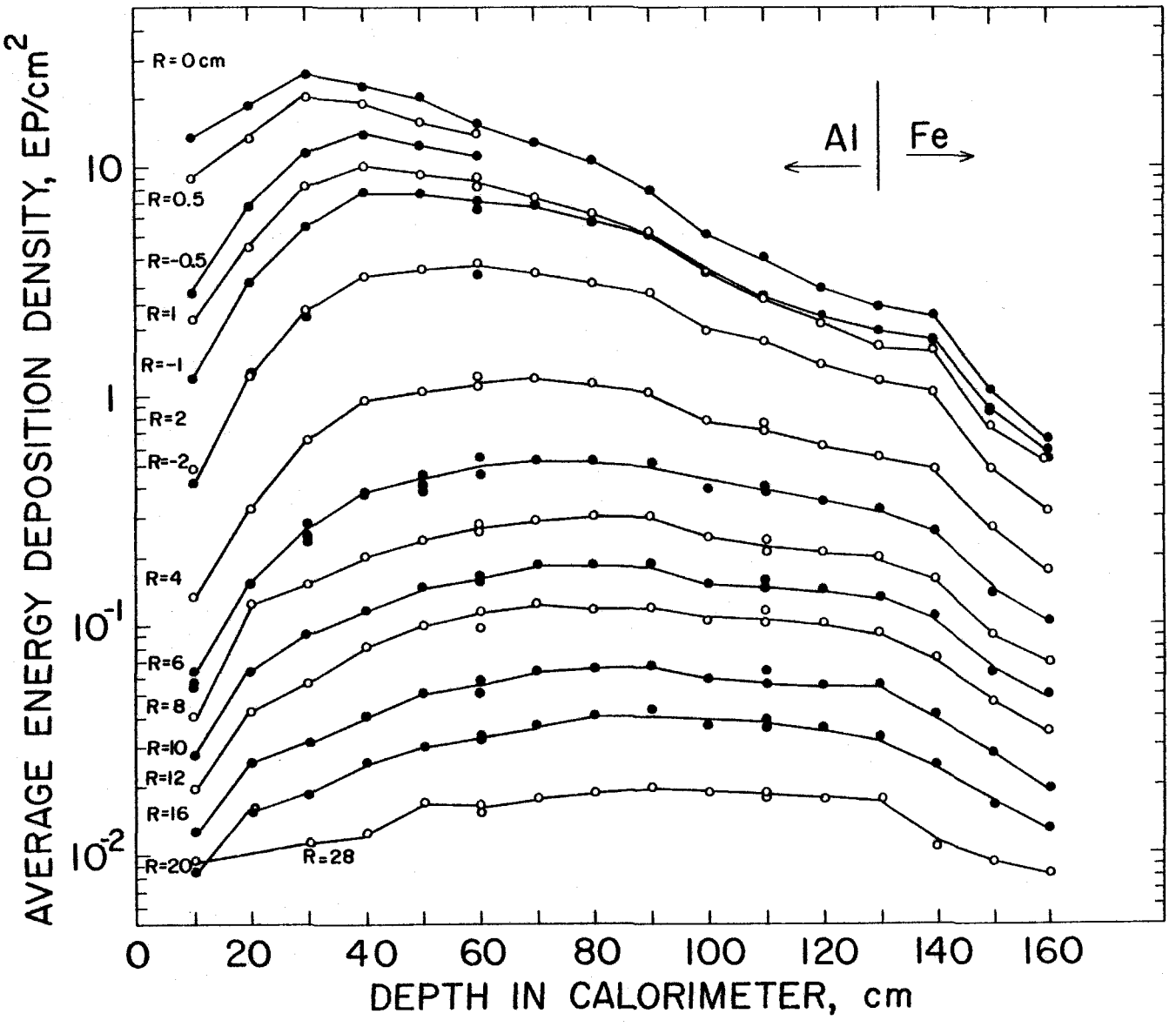

FIG. 6(a).

6. Longitudinal shower development curves for (a) Al, (b) Fe, and (c) Pb. The lines between the data points are drawn to guide the eye. The semilogarithmic scale allows the full range of the data to be displayed. The horizontal scales are approximately equal for all three graphs when depth is measured in interaction lengths. The break in the curves in (a) at large depth is due to a transition between the Al under study and some Fe plates behind it.

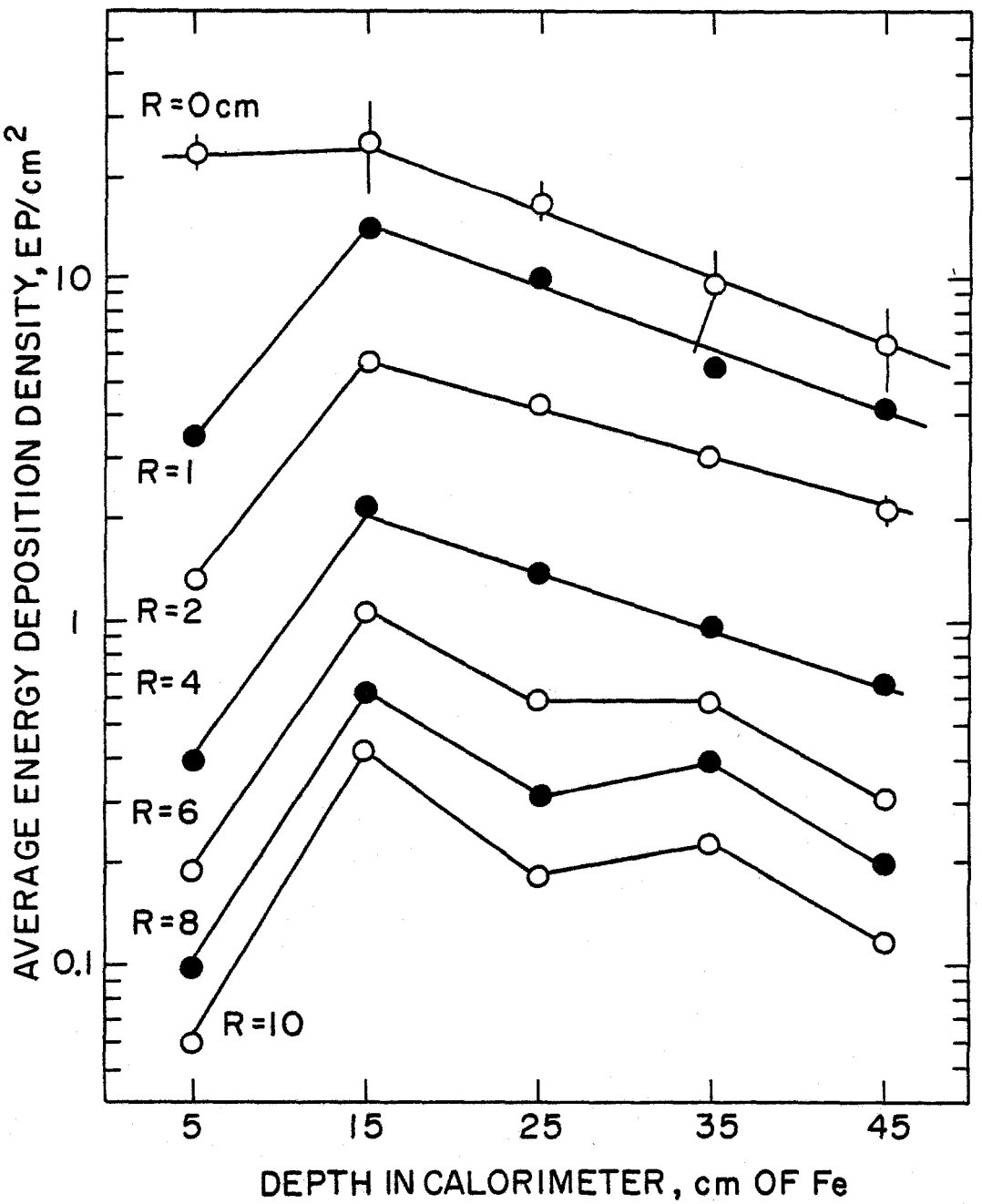
R=0cm
R=1
R=2
R=4
R=6
R=8
R=10
10
1
0.1
AVERAGE ENERGY DEPOSITION DENSITY, EP/cm²
5
15
25
35
45
DEPTH IN CALORIMETER, cm OF Fe

FIG 6(b).

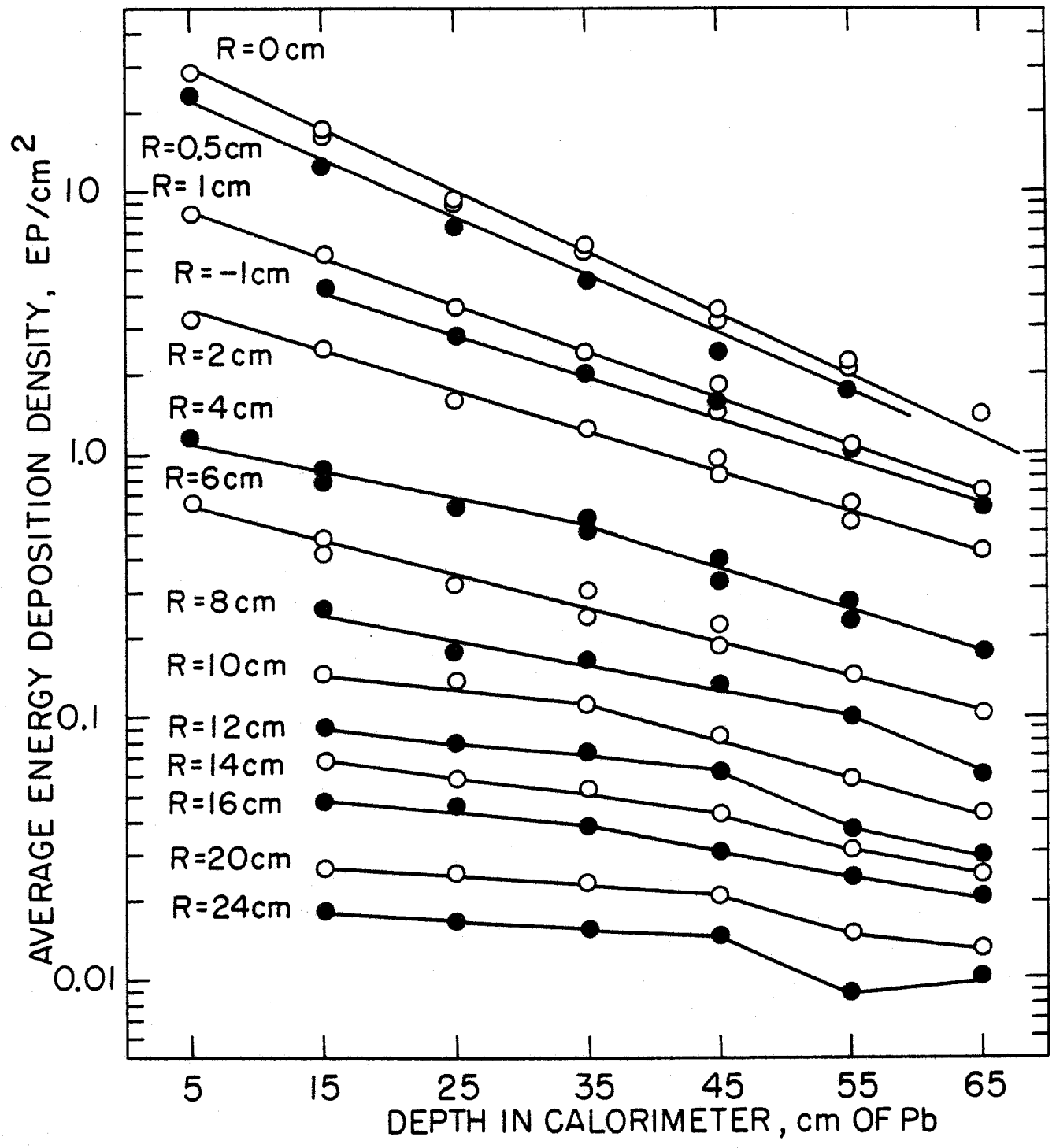
R=0 cm
R=0.5cm
R= 1cm
R= -1cm
R=2 cm
R=4 cm
R=6cm
R=8 cm
R=10cm
R=12cm
R=14cm
R=16cm
R=20cm
R=24cm
AVERAGE ENERGY DEPOSITION DENSITY, EP/cm2
10
1.0
0.1
0.01
5
15
25
35
45
55
65
DEPTH IN CALORIMETER, cm OF Pb

FIG. 6(c).

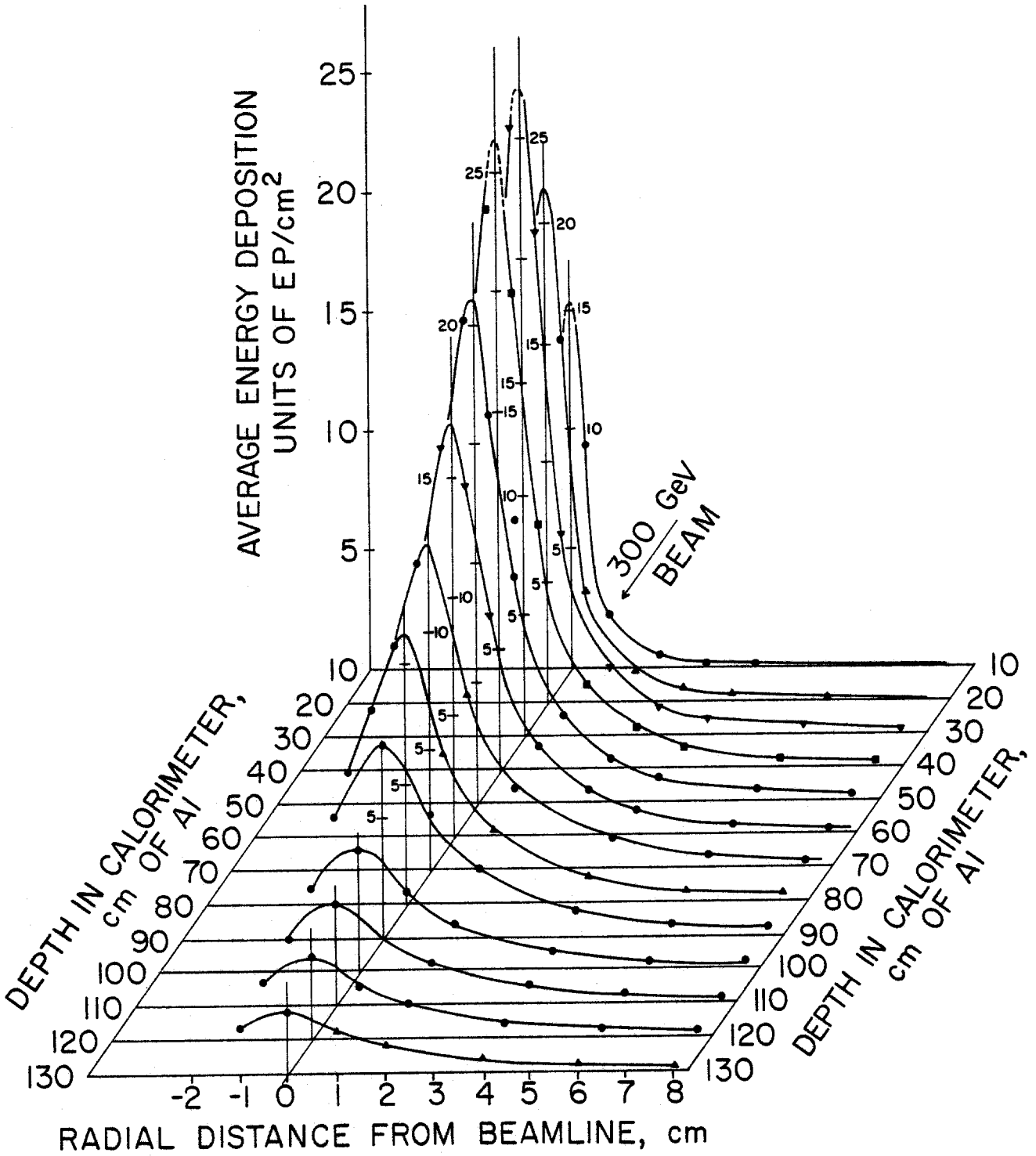

FIG. 7(a)

7. Cascade profile curves for (a) Al and (b) Pb. The average energy deposition per shower (units of EP/cm^2) is shown as a function of radial distance from the beamline for constant values of depth in the calorimeter. The linear scales used clearly show the sharpness of the peaks at small radii but do not clearly show the sensitivity of the measurements at large radii. The scales of the two graphs are approximately equal when distances are measured in interaction lengths. Buildup in the Pb dump is not visible with this coarse a sampling interval. (Most data points in this figure have been shifted by 1 to 3 mm to correct for a systematic misalignment.)

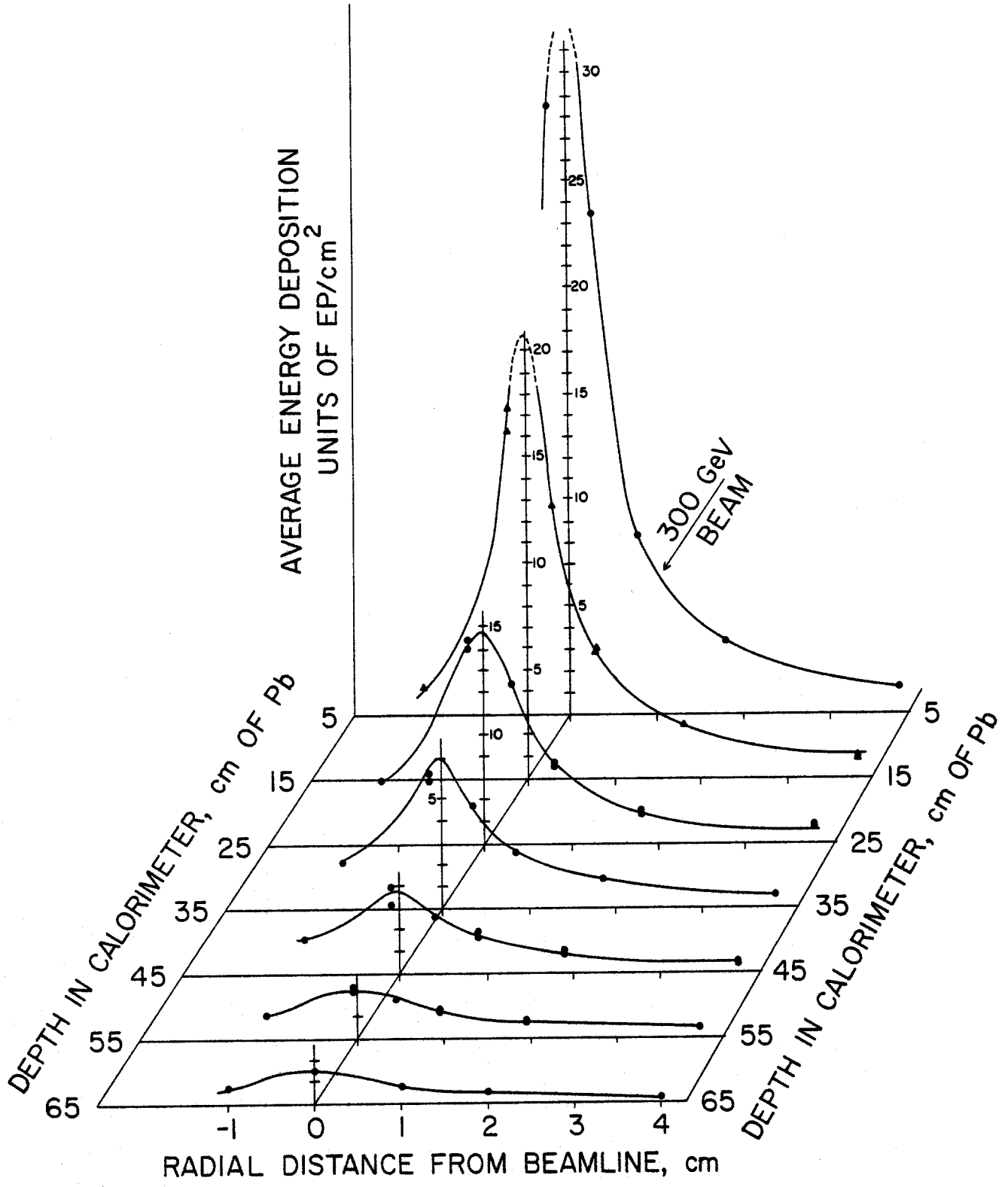
AVERAGE ENERGY DEPOSITION
UNITS OF EP/cm^2
300 GeV
BEAM
DEPTH IN CALORIMETER, cm OF Pb
RADIAL DISTANCE FROM BEAMLINE, cm
5
15
25
35
45
55
65
-1
0
1
2
3
4
30
25
20
15
10
5

FIG. 7(b).

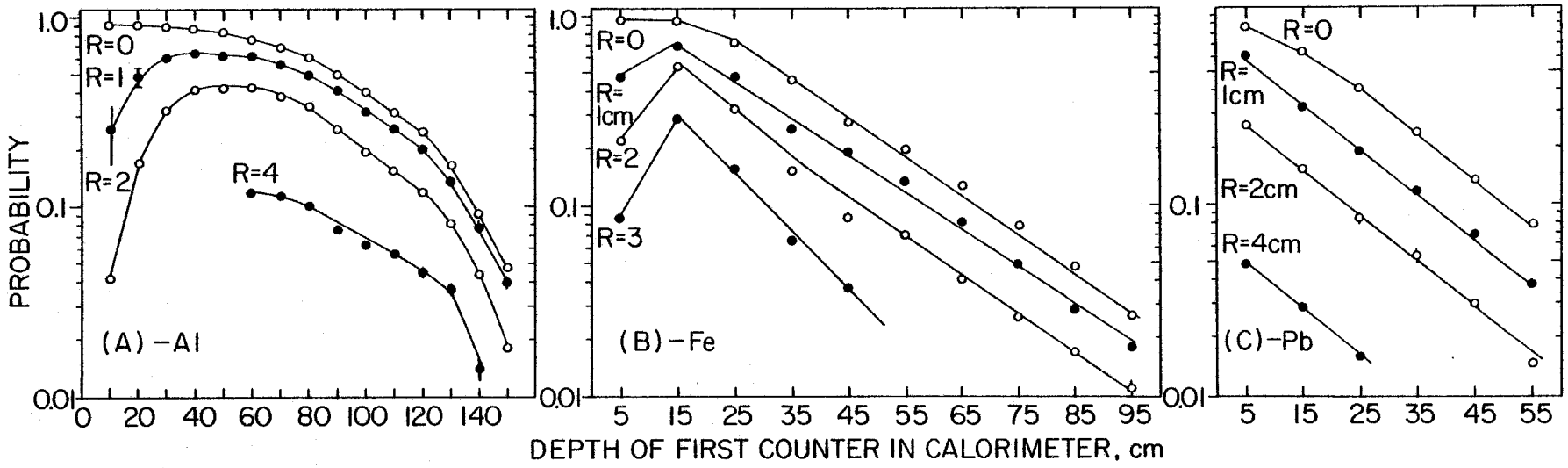

8. The probability for a given radius and material that a shower will produce large signals ($\geq$ 0.8 EP) in two successive fingers, for the (a) Al, (b) Fe, and (c) Pb calorimeters. The lines between the data points have been drawn to guide the eye.